Technical Paper

ISSN 1997-1400 Int. J. Pavement Res. Technol. 6(3):155-164

Artificial Neural Network Models to Estimate Resilient Modulus of Cementitiously Stabilized Subgrade Soils

Pranshoo Solanki[1+]

Abstract: A combined laboratory and modeling study was undertaken to develop a database for cementitiously stabilized subgrade soils in Oklahoma and to develop artificial neural network (ANN) models that could be used to estimate resilient modulus (M_r) from commonly used subgrade soil properties in Oklahoma. An M_r database was developed using laboratory test results on 160 specimens prepared by using four soils stabilized with three cementitious additives, namely, lime (3%, 6% and 9%), class C fly ash (CFA) (5%, 10% and 15%) and cement kiln dust (CKD) (5%, 10% and 15%). One Multi-Layer Perceptrons Network (MLPN) and one Radial Basis Function Network (RBFN) types of ANN models were developed using a development dataset and validated using a different dataset. Overall, MLPN neural network was found to show best acceptable performance for the present evaluation and validation datasets.

DOI:10.6135/ijprt.org.tw/2013.6(3).155

Key words: *Artificial neural network; Cement kiln dust; Cementitious Stabilization; Fly ash; Resilient modulus; Subgrade.*

Introduction

Empirical design methods for flexible pavement structures are primarily based on the equations that were developed largely from the AASHO Road Tests conducted in the1950's. These methods fail to reflect the dynamic nature of traffic loads. Therefore, the mechanistic design methods referred to as the "AASHTO Guide for Design of Pavement Structure" [1] recommended the use of resilient modulus (Mr), a dynamic-strength parameter, to characterize flexible pavement materials. The Mr accounts for the cyclic nature of vehicular traffic loading, and is defined as the ratio of deviatoric stress to recoverable strain.

Several laboratory and field procedures are currently either being used or evaluated for determining a design Mr value for subgrade soil. Direct laboratory methods used for evaluating Mr during the past two decades include resonant column, torsional shear, gyratory, and repeated load triaxial testing [1-4]. Among these, the Mr from repeated load triaxial test (RLTT) is used most frequently because of the repeatability of the test results and its representation of field stress in a controlled laboratory environment. RLTT is conducted in the laboratory on remolded or undisturbed samples according to different AASHTO test methods of which AASHTO T307 is used frequently [5]. The AASHTO T307 test method can be a time consuming and expensive test method, particularly for small projects.

In the 2002 AASHTO design guide, a hierarchical approach is used to determine different design inputs including Mr [5]. It requires evaluation of pertinent engineering properties of subgrade soils in the laboratory or field to pursue a Level 1 (most accurate) design. However, for a Level 2 (intermediate) design the inputs are user selected, possibly from an agency database or from a limited testing program or could be estimated through correlations [5]. A Level 3 design, which is the least accurate and generally not recommended, uses only the default values. For Level 2 designs, a regression model for Mr can be very useful as it provides the designer with significant flexibility in obtaining the design inputs for a project.

Since conducting Mr test in the laboratory is tedious and time consuming, regression models are generally preferred to estimate the Mr value. Several studies have previously been undertaken to develop empirical correlations for estimating Mr values in terms of other soil properties [6-12]. However, only a few models and correlations are available for cementitiously stabilized soils in the literature; these correlations are either limited to one type of additive [13-15] or applicable only for a particular stress level [5, 16-18]. One of the reasons for limited number of regression models for cementitiously stabilized soils is poor performance of regression relationship between Mr values and soil/additive properties at different stress levels.

Consequently, the primary objective of the study presented herein is to develop artificial neural network (ANN) models for Mr from some common subgrade soils in Oklahoma, stabilized with locally available cementitious additives for Level 2 pavement design applications. The strengths and the weaknesses of the developed models were examined using additional Mr test results that were not used in the development of these models. The models developed in this study are expected to be useful in the Level 2 designs of pavements in Oklahoma.

Review of Previous Studies

ANN has become an important modeling technique due to its success in many engineering applications including geotechnical engineering problems [see e.g., 19-21]. One of the common artificial neural networks currently in use is the feed-forward network. As evident from its name, a feed-forward network only allows the data flow in the forward direction [23-26]. Based on the architecture, a number of feed-forward networks are available such as multi-layer perceptron, radial basis function, probabilistic neural

[1] Department of Technology, Illinois State University, Campus Box 5100, Normal, Illinois, 61780, USA.

[+] Corresponding Author: E-mail psolanki@ilstu.edu
Note: Submitted May 25, 2012; Revised December 23, 2012; Accepted December 24, 2012.

networks, generalized regression neural networks, and linear networks [19, 21, 27-29].

ANN contains a number of simple, highly interconnected processing elements, known as "nodes" or "units." In a typical processing element, each input connection has a weighting value. With the weighting value, input data and bias value, a net input is described into the processing element. Then, a transfer function provides an output from the net input. Finally, a single output is produced and transmitted to other processing elements [20, 30-31].

The weights between the processing elements are adjusted during the "training or learning" phase. In the training process, a number of epochs are performed in the network. After each epoch, the weights are adjusted and a sum of mean squared error between target and output values is calculated. The training process stops when the sum of mean squared error is minimized or falls within an acceptable range [21, 31].

Different algorithms can be used to train a network. In general, the training algorithms can be divided into two types: supervised and unsupervised. The supervised algorithms adjust the weights and the thresholds using the input and target output values, while the unsupervised algorithms use only the input values. The supervised training algorithms include back propagation, conjugate gradient descent, Levenberg-Marquardt, Pseudo-inverse, etc. [21, 27, 31].

A number of researchers have utilized ANN technique in pavement applications. For example, Meier et al. [32] augmented a computer program, WESDEF, with ANN models to back-calculate pavement layer moduli. The ANN models were trained to compute the layer Mr from falling weight deflectometer (FWD) data from flexible pavements [32].

In another pavement application study, Sharma and Das [28] used ANN models to back-calculate layer moduli with better accuracy compared with other software, namely, EVERCALC and ExPaS. In a recent study, Far et al. [28] utilized ANN for estimating the dynamic modulus of asphalt concrete. The results showed that the predicted and measured dynamic modulus values are in close agreement using ANN models.

Ceylan et al. [33] used ANN models for predicting dynamic modulus of hot mix asphalt. The ANN-based models showed better overall prediction accuracy as compared regression models. The ANN models also produced better agreement between predicted and measured rutting and cracking of a pavement.

Xiao et al. [34] used the ANN approach in estimating the stiffness behavior of rubberized asphalt concrete containing reclaimed asphalt pavement. In another study, Xiao et al. [35] developed an ANN model for predicting the viscosity of crumb rubber modified binders using four input variables: asphalt binder source, rubber size, mixing duration, and rubber content.

In another study by Far et al. [36], ANN models for estimating dynamic moduli of LTPP sections were developed. A large national data set that covers a substantial range of potential input conditions was utilized to train and verify the ANNs. First, the ANN predictive models were trained and ranked using a common independent data set that was not used for calibrating any of the ANN models. A decision tree was developed from these rankings to prioritize the models for any available inputs. Next, the models were used to estimate the dynamic moduli for the LTPP database materials and ultimately to characterize the master curve and shift factor function. It was found that ANN models predict reliable dynamic moduli of LTPP sections over a wide range of temperatures and frequencies.

In a recent study, Thube [37] developed ANN based pavement deterioration models for low volume pavements in India. A database containing distresses, subgrade characterization and traffic data were collected from 61 in-service pavement sections over a three year period was developed. A total of four unified ANN based models were suggested for predicting cracking, raveling, rut depth, and roughness progression of low volume pavements.

Characteristics of Soils and Database

In this study, a total of four clay subgrade soil series namely, Port series (P-soil), Vernon series (V-soil), Carnasaw series (C-soil) and Kingfisher series (K-soil) are used. Of these, three soils (P-, V- and C-soil) were used in the development/evaluation of models and are collectively referred to as the "development/evaluation dataset." The remaining soil (K-soil) was used for the validation of the models. Data for stabilized K-soil is collectively referred to as the "validation dataset." P-soil, V-soil, C-soil and K-soil are CL-ML, CL, CH and CL clays, respectively, in accordance with the Unified Soil Classification System (USCS). A total of three locally available additives, namely, hydrated lime, class C fly ash (CFA), and cement kiln dust (CKD) were used in this study. The physical and chemical properties of soils and additives are presented in Tables 1 and 2, respectively.

An Mr database developed using laboratory test results on 160 specimens was prepared by using four soils stabilized with three additives namely, lime (3%, 6% and 9%), CFA (5%, 10% and 15%) and CKD (5%, 10% and 15%). An outlier approach was used employing t-statistics to discard the test results if a sample result deviated significantly from the average of Mr results obtained from the four replicates. The critical value (t-critical) for student's t-test is taken at a significance level (α) of 0.05. If the calculated t-statistic value is greater or equal to this value (t-critical), then there is a one in twenty chance that the value is from the same population. Additional details about statistical parameters such as standard deviation and coefficient of variation are provided elsewhere [38].

Artificial Neural Network Models

Development and Evaluation of Models

In the present study, two feed-forward-type ANN models, namely, Radial Basis Function Network (RBFN) and Multi-Layer Perceptrons Network (MLPN), were developed using the Mr dataset of P-, V- and C-soils. Previous studies show that RBFN and MLPN are the two best ANN models for predicting Mr values in subgrade soils [22]. A commercial software, STATISTICA 8, was used to develop these models. In the present application, the input layer consists of 25 nodes (or neurons), one node for each of the independent variables, namely, UCS/Pa (unconfined compressive strength/atmospheric pressure), MC (moisture content), DUW/γw (dry unit weight/unit weight of water), P_{200} (passing No. 200 sieve), PI (plasticity index), CC (clay content), pHs (pH of soil), SSAs (specific surface area of soil), CECs (cationic exchange capacity of soil), PA (percentage of additive), SiO_2 (silica content), Al_2O_3

Table 1. Testing Designation and Soil Properties.

Method	Parameter/Units	P-soil	K-soil	V-soil	C-soil
ASTM D 2487	USCS Symbol	CL-ML	CL	CL	CH
AASHTO M 145	AASHTO Designation	A-4	A-6	A-6	A-7-6
ASTM D 2487	USCS Name	Silty Clay with Sand	Lean Clay	Lean Clay	Fat Cay
ASTM D 2487	% Finer than 0.075 mm	83	97	100	94
ASTM C 430	% Finer than 0.045 mm	54	89	95	87
ASTM D 422	% Finer than 0.002 mm (Clay Content)	11	45	39	48
ASTM D 4318	Liquid Limit	27	39	37	58
ASTM D 4318	Plastic Limit	21	18	26	29
ASTM D 4318	Plasticity Index	5	21	11	29
…	Activity	0.24	0.47	0.28	0.69
ASTM D 854	Specific Gravity	2.65	2.71	2.61	2.64
ASTM D 698	Optimum Moisture Content (%)	13.1	16.5	23.0	20.3
ASTM D 698	Max. Dry Unit Weight (kN/m^3)	17.8	17.4	16.0	16.3

USCS: Unified Soil Classification System

Table 2. Chemical and Physical Properties of Soils used in this Study.

Chemical Compound/Property	Percentage by Weight, (%)			
	P-soil	K-soil	V-soil	C-soil
Silica (SiO_2)[a]	77.7	65.8	54.0	63.4
Alumina (Al_2O_3)[a]	7.4	13.0	17.6	21.5
Ferric Oxide (Fe_2O_3)[a]	2.3	4.8	7.2	9.1
Silica/Sesquioxide Ratio (SSR) $SiO_2/(Al_2O_3+Fe_2O_3)$	14.9	7.0	4.1	3.9
Calcium Oxide (CaO)[a]	3.1	3.6	3.8	0.1
Magnesium Oxide (MgO)[a]	1.9	3.5	5.0	1.2
Sulfur Trioxide (SO_3)[a]	0.0	0.1	1.8	0.0
Alkali Content ($Na_2O + K_2O$)[a]	2.4	3.2	5.8	3.0
Percentage Passing No. 325[b]	54.0	88.8	94.8	87.2
pH (Pure Material)[c]	8.91	8.82	8.14	4.17
Sulfate Content (ppm)[d]	< 40	< 40	15,400	267
Specific Surface Area (m^2/gm)[e]	51.0	92.5	116.5	118.5
Cation Exchange Capacity (meq/100 gm)[f]	11.5	21.7	19.9	5.2
28-day UCS (kPa)	224	191	168	207

[a]X-ray Fluorescence analysis; [b]ASTM C 430; [c]ASTM D 6276; [d]OHD (Oklahoma Highway Department) L-49 test method, which is the Method of Test for Determining Soluble Sulfate Content in Soil; [e]Ethylene glycol monoethyl ether method [39]; [f]EPA 9081 test method; No. 325: 0.045 mm

(alumina content), Fe_2O_3 (iron content), SSR_a (silica sesquoxide ratio of additive), CaO (calcium oxide), MgO (magnesium oxide), ACA (alkali content of additive), FL (free lime content), LOI (loss on ignition), P_{325} (percent passing No. 325 sieve), pH_a (pH of additive), SSA_a (specific surface area of additive), SSR_m (silica sesquoxide ratio of soil-additive mix), σ_3/P_a (confining pressure/atmospheric pressure), and σ_d/P_a (deviatoric pressure/atmospheric pressure). The output layer consists of one node, representing Mr/P_a. For each ANN model developed, a trial and error approach was used to find the number of nodes in the hidden layer(s), in search of the optimal model. After the architecture was set, the development dataset was fed into the model for training. To examine the strengths and weaknesses of the developed models, they were evaluated by comparing the predicted Mr values with the experimental values (or measured values) with respect to the R^2 values. Thus, a higher R^2 value was considered a better fit of the evaluation dataset. Previously, several researchers have used R^2 as an indicator of model performance [40-41].

Radial Basis Function Network (RBFN)

The radial basis function network (RBFN) divides the modeling space using hyperspheres. The centers and radii are used to characterize these hyperspheres. The RBFN units respond non-linearly to the distance of points from the center represented by a radial unit. The response surface of a single radial unit is the Gaussian (bell-shaped) function, peaked at the center, and descending outwards [26, 43-44]. Therefore, the RBFN has three layers: input, hidden, and output. The hidden layer consists of radial units. It models the Gaussian response surface. The two most common methods for assigning the center of the radial units are sub-sampling and K-Means algorithm [26, 41].

The RBFN model has one hidden layer. A trial and error approach was used to determine the optimal number of nodes in the hidden layer. Following this approach, the optimal number of nodes in the hidden layer producing the least root mean square error (RMSE), was found to be 18, as shown in Fig. 1. The R^2 value of the RBFN

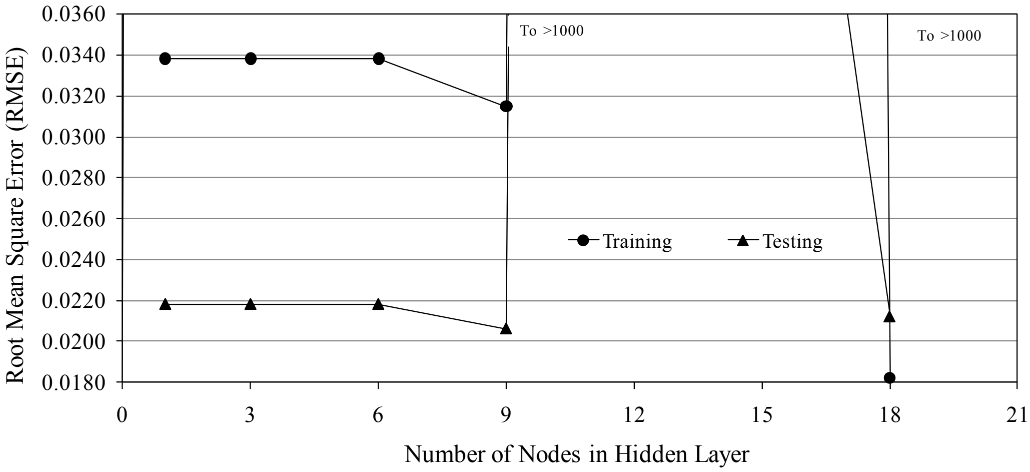

Fig. 1. Selection of Number of Nodes in Hidden Layer (RBFN) for Training and Testing Sets.

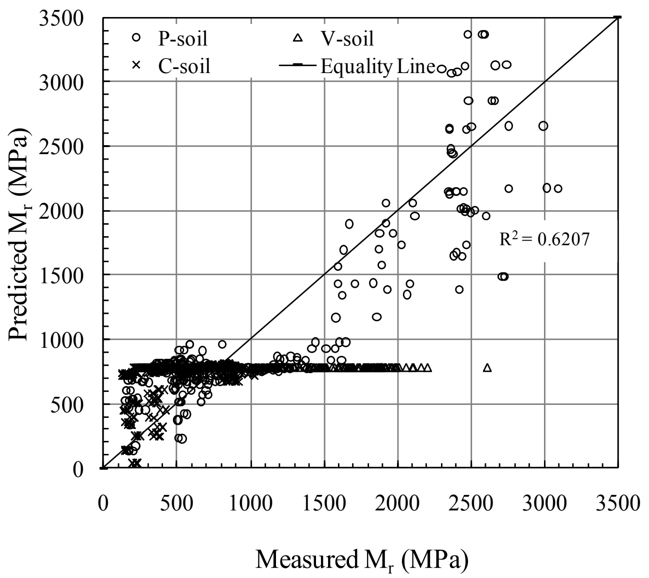

Fig. 2. Predicted Mr Versus Measured Mr for P-, V- and C-soil using RBFN 25-18-1 Neural Network Model.

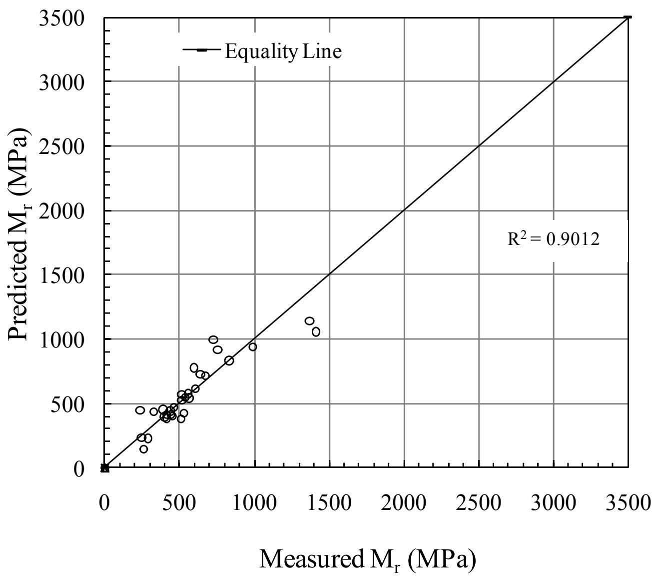

Fig. 3. Predicted Mr Versus Measured Mr for Two Mr Tests: 3% lime-stabilized P-soil and 5% CKD-stabilized V-soil using RBFN 25-10-1 Neural Network Model.

model is 0.6207, which is the lowest among all the statistical and ANN models used in this study. Fig. 2 shows an overall comparison between measured and predicted Mr values for this model. Significant scatter is observed for the entire data range, justifying a low R^2 value. Based on these results, it is clear that RBFN is incapable of predicting the development dataset. However, the R^2 value for fewer specimens is close to 1. For example, predicted Mr values show a good correlation ($R^2 = 0.9012$) with experimental Mr values for 3% lime-stabilized P-soil and 5% CKD-stabilized V-soil specimens, as shown in Fig. 3. The correlation becomes weaker as more soil and additives types are included in the dataset.

Multi-Layer Perceptrons Network (MLPN)

The MLPN is one of the popular network architectures in use today [22, 44-46]. The MLPN consists of an input layer, a number of hidden layers, and an output layer. In each of the hidden layers, the number of nodes (also called neuron) can be varied. Due to the number of layers and the number of nodes in each layer, the MLPN can adjust the architecture of the network based on the complexity of the problem. In STATISTICA 8.0, the MLPN has up to three hidden layers available. Each of the nodes in the network performs a biased weighted sum of their inputs and passes this activation level through a transfer function to produce its output. The weights and biases in the network are adjusted using a training algorithm. The training algorithms available in STATISTICA 8 are back propagation, gradient descent, conjugate gradient, and quasi-Newton [26].

In MLPN, the weighted sum of input components is calculated as [44-45]:

$$S_j = \sum_{i=0}^{n} W_{ij} x_i + Q_i \tag{1}$$

where i is the number of inputs, j is the number of neurons in the

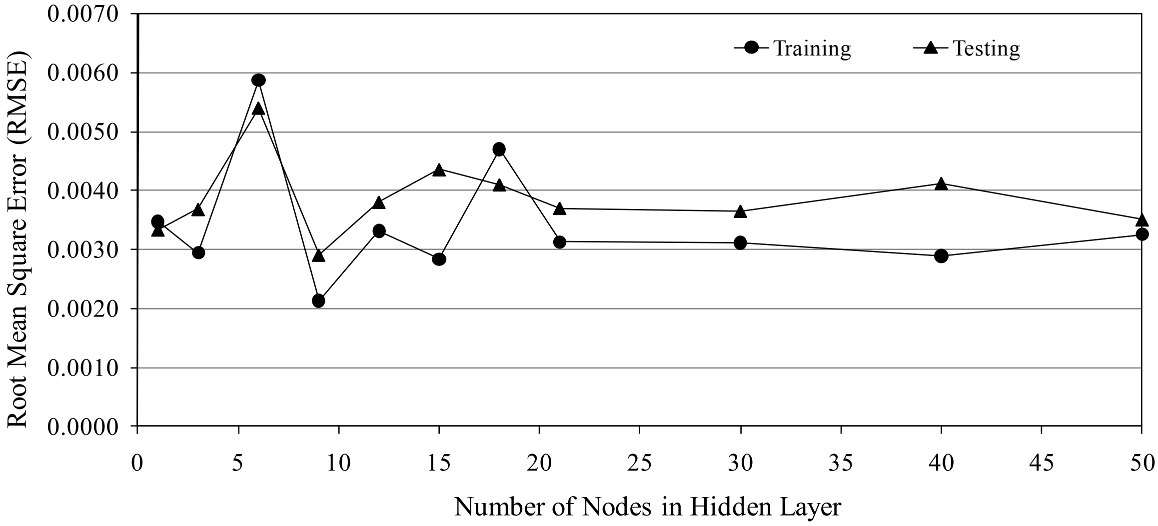

Fig. 4. Selection of Number of Nodes in Hidden Layer (MLPN) for Training and Testing Sets.

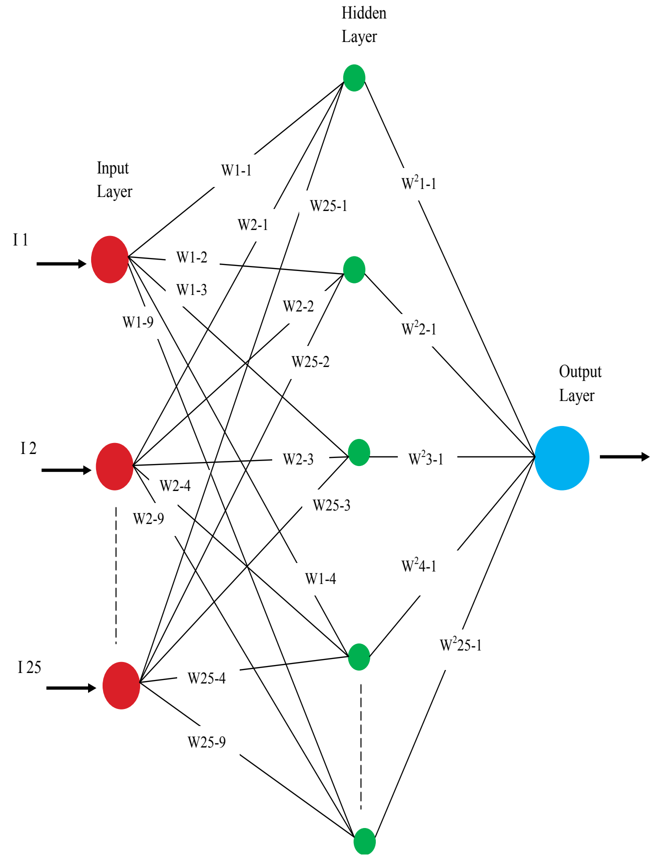

Fig. 5. Neural Network Architecture of MLPN 25-9-1.

hidden layers, S_j is the weighted sum of the jth neuron for the input received from the preceding layer with n neurons (or inputs for MLPN with one hidden layer), W_{ij} is the weight between the jth neuron and the ith neuron in the preceding layer, xi is the output of the ith neuron in the preceding layer (or inputs for MLPN with one hidden layer), and Q_i is the constant bias term. Once the weighted sum S_j is computed, the output of the jth neuron y_j is calculated with an activation function, sigmoid in this case, as follows:

$$y_i = f(S_j) = \frac{1}{1+\exp(-\eta S_j)} \quad (2)$$

where η is a constant used to control the slope of the semi-linear region. The sigmoid nonlinearity activates in every layer except the input layer [45-46].

In the present study, the MLPN model was developed with one hidden layer. The number of nodes in the hidden layers was selected, as nine, based on minimum RMSE by using a trial and error approach, as shown in Fig. 4. The architecture of the developed MLPN model is illustrated in Fig. 5. The neurons of the input layer receive information from outside the environment and transmit to the neurons of the hidden layer, without performing any calculation. Then, the hidden layer processes the incoming information and extracts useful features to construct the mapping from the inputs space and interconnects each other through weights. The neuron of last layer, called the output layer, produces the network prediction to the outside world in the form of Mr values.

The training algorithm used in the study is the conjugate gradient algorithm, activation function is sigmoid function, and number of epochs is 5,000, producing an error of less than 10^{-6} per 100 cycles. As a result of the training, the network produced 9 x 25 weights (W) and 9 bias values (Q_i) connecting input and hidden layer, 9 x 1 weights (W2) and 1 bias value (Q) connecting hidden layer and output layer. Table 3 presents a list of the final weights and bias values. With these weights and bias values, the network is able to simulate Mr values with the trained data and to predict Mr values with the untrained data by using following equations:

$$\frac{M_r}{P_a} = \frac{30.54}{1+\exp\left(\frac{1.4071}{1+e^{-F_1}} + \frac{0.6943}{1+e^{-F_2}} + \frac{0.7252}{1+e^{-F_3}} + \frac{1.3595}{1+e^{-F_4}} + \frac{0.4442}{1+e^{-F_5}} - \frac{0.3108}{1+e^{-F_6}} - \frac{0.2729}{1+e^{-F_7}} - \frac{0.7253}{1+e^{-F_8}} + \frac{0.6157}{1+e^{-F_9}}\right)} \quad (3)$$

Table 3. Weight and Bias Values for MLPN 25-9-1.

Weights (ij)	Number of Hidden Layer Neurons (j)								
	1	2	3	4	5	6	7	8	9
				Between Input and Hidden Layer					
W_{1j} (UCS/P_a)	0.7849	-0.2768	-0.4757	-0.7488	-0.3004	-0.6057	-0.2175	-0.6374	-0.5808
W_{2j} (MC)	-0.2339	-0.3610	-0.4485	-0.3660	0.1410	0.0192	-0.3717	-0.2784	-0.0769
W_{3j} (DUW/γ_w)	0.1414	0.0763	0.1269	0.0510	0.3162	-0.4473	-1.9853	-1.0919	0.9099
W_{4j} (P_{200})	-0.1455	0.2050	-0.6296	-0.3227	-0.0140	0.2394	-0.0842	-0.6616	-0.0189
W_{5j} (PI)	-0.1268	-0.0302	0.4097	-0.0823	-0.0651	0.1827	-0.2170	0.0563	-0.0482
W_{6j} (CC)	0.0414	-0.0964	0.0139	-0.0245	-0.1234	0.5100	-0.2283	0.1011	0.3436
W_{7j} (pH_s)	0.6026	0.6030	-0.1112	0.4181	0.0286	0.5532	0.2384	0.2701	0.2605
W_{8j} (SSA_s)	0.0932	-0.0469	0.2761	0.2811	-0.0070	0.0062	-0.0125	-0.0087	-0.0044
W_{9j} (CEC)	-0.1407	0.5116	1.4874	0.7090	0.1179	0.2400	-0.1110	0.4663	0.3095
W_{10j} (PA)	0.3427	-0.4081	0.5317	0.5927	-0.1045	-0.1115	-0.0787	-0.0072	-0.0460
W_{11j} (SiO_2)	-0.0769	-0.0565	-0.0937	-0.0767	-0.0852	-0.0178	-0.0697	0.0973	0.0112
W_{12j} (Al_2O_3)	0.2679	0.0830	0.2180	0.3672	-0.1492	0.1319	0.0133	-0.1156	-0.2717
W_{13j} (Fe_2O_3)	0.0508	0.8503	-0.1267	-0.1323	-0.1328	0.0454	-0.2398	-0.1594	-0.1061
W_{14j} (SSR_a)	-0.3170	-0.2456	-0.2431	-0.2376	-0.2884	-0.0872	0.0412	0.6130	-0.0230
W_{15j} (CaO)	-0.0830	-0.0955	-0.2227	0.0881	-0.0618	0.1889	-0.3144	0.0350	0.4890
W_{16j} (MgO)	-0.0860	0.0378	-0.0123	-0.4499	0.1731	0.0169	-0.2102	0.3254	0.0249
W_{17j} (ACC)	0.1233	0.0478	0.1394	0.1016	0.0063	-0.1280	0.2603	0.4927	-1.0806
W_{18j} (FL)	0.6707	-1.5454	-0.7059	0.0926	0.8779	0.0639	0.4461	0.1220	0.2625
W_{19j} (LOI)	0.2201	-0.7126	0.0994	0.2387	-0.2065	0.3945	-0.1745	-0.0968	-0.1482
W_{20j} (P_{325})	0.0653	-0.5064	-0.0065	0.2077	-2.7049	-0.6988	0.1553	0.2068	-0.3732
W_{21j} (pH_a)	-0.1558	-0.0510	0.2445	-0.0054	0.6924	0.0392	-0.1549	-0.0408	0.9005
W_{22j} (SSA_a)	-0.1839	-0.0622	0.4394	-0.5280	0.1013	-0.0296	0.0777	-0.1034	0.0928
W_{23j} (SSR_m)	0.0014	0.2497	0.0841	-0.3350	-0.3646	-0.1201	-0.1905	-0.2597	-0.3332
W_{24j} (σ_3/P_a)	0.2257	-0.6296	-0.3056	0.1483	0.1646	0.1695	0.0118	0.1503	0.1561
W_{25j} (σ_d/P_a)	0.1277	0.1610	0.1236	0.1076	0.0899	0.1620	0.0953	0.0014	-0.5593
Bias Q_j	-0.3421	-0.0373	0.2645	-0.1617	-0.3442	0.0294	0.0885	-0.0228	0.2484
				Between Hidden and Output Layer					
W^2_j (M_r/P_a)	1.4071	0.6943	0.7252	1.3595	0.4442	-0.3108	-0.2729	-0.7253	0.6157
Bias Q	0.6435								

where,

$$
\begin{aligned}
F_1 = {} & W_{1-1}\left(\frac{UCS}{P_a}\right)+W_{2-1}(MC)+W_{3-1}\left(\frac{DUW}{\gamma_w}\right)+W_{4-1}(P_{200}) \\
& +W_{5-1}(PI)+W_{6-1}(CC)+W_{7-1}(pH_s)+W_{8-1}(SSA_s) \\
& +W_{9-1}(CEC)+W_{10-1}(PA)+W_{11-1}(SiO_2)+W_{12-1}(Al_2O_3) \\
& +W_{13-1}(Fe_2O_3)+W_{14-1}(SSR_a)+W_{15-1}(CaO) \\
& +W_{16-1}(MgO)+W_{17-1}(ACA)+W_{18-1}(FL)+W_{19-1}(LOI) \\
& +W_{20-1}(P_{325})+W_{21-1}(pH_a)+W_{22-1}(SSA_a) \\
& +W_{23-1}(SSR_m)+W_{24-1}\left(\frac{\sigma_3}{P_a}\right)+W_{25-1}\left(\frac{\sigma_d}{P_a}\right)+Q_1
\end{aligned}
\tag{4}
$$

Functions F_2, F_3,…, F_9 can be obtained by employing weights $W_{i\text{-}2}$, $W_{i\text{-}3}$, …, $W_{i\text{-}9}$ (i = 1 – 25), respectively in Eq. (4). By employing the aforementioned approach, the R^2 value of the MLPN model was found to be 0.9872, indicating that the MLPN model is expected to better correlate to the Mr values than the RBFN (0.6207) model. Fig. 6 shows a comparison between the experimental and predicted values of Mr values for the MLPN model. It is clear that the level of scatter in data points reduced significantly for this model. It is also evident that the predicted values are closer to the equality line.

Validation of Models

As noted earlier, a different dataset of Mr values of stabilized V-soil specimens was used for validation. This provides different views on the prediction quality and the importance of datasets on regression analysis [42, 47-48]. Additionally, a comparison was made between the differences in the R^2 values of the development/evaluation dataset and the validation dataset.

The RBFN model predicted the Mr values of the validation dataset with a low R^2 value of 0.3172. Fig. 7 shows a comparison of the prediction quality of the RBFN model for the validation dataset. It is observed that the data points start to deviate to a “banded” distribution ranging between approximately 700 – 1000 MPa, as shown in Fig. 7. The effect is presented as a narrow horizontal band indicating a poor prediction. Also, Se/Sy values of greater than 1 indicate low quality of Mr prediction achieved by using the RBFN model. On the other hand, the R^2 of the validation dataset for the MLPN model was found to be 0.9582 (Fig. 7). The corresponding Se/Sy value for the MLPN model was found to be less than 1 (0.5985). It is also evident from Fig. 7 that the scatters for the

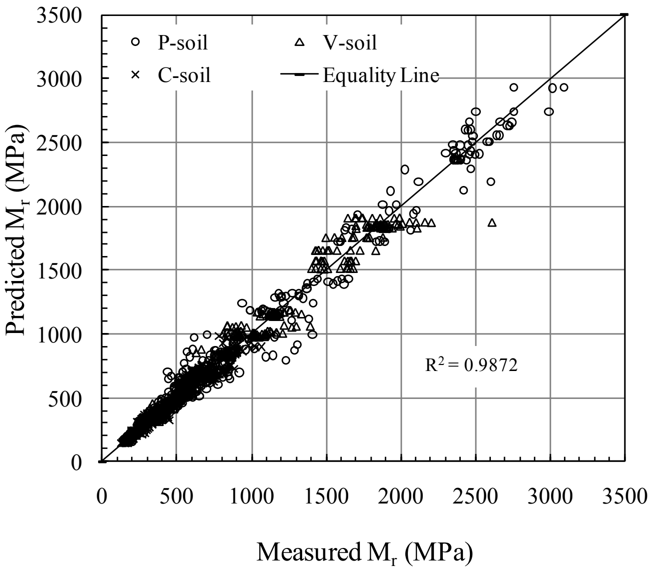

Fig. 6. Predicted Mr Versus Measured Mr for P-, V- and C-soil using MLPN 25-9-1 Neural Network Model.

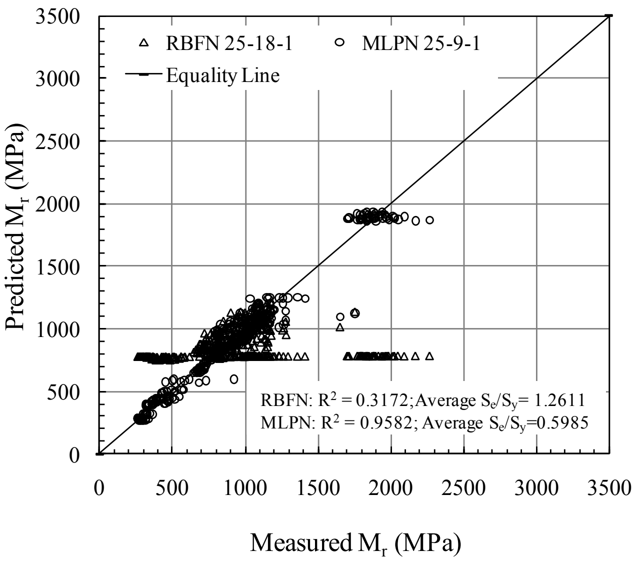

Fig. 7. Predicted Mr Versus Measured Mr for K-soil Using RBFN 25-18-1 and MLPN 25-9-1 Neural Network Models.

MLPN model are closer to the equality line as compared to the scatter of the RBFN model. Overall, the MLPN model appears to be the best model for the present (development/evaluation and validation) datasets.

Sensitivity Analysis

A sensitivity study was conducted on the best performing MLPN model to evaluate the effect of each independent variable. In pursuing this sensitivity analysis, only one independent variable was changed at a time. First, the average and standard deviation of each independent variable were determined from the combined evaluation/development and validation datasets. The corresponding results of the mean and standard deviation of each independent variable for MLPN model is shown in Table 4. Then, Mr value was calculated by inputting the average values of each independent variable into the corresponding models and this calculated value was called the "primary Mr value." A series of Mr values were then calculated by changing (within plus and minus of one-half standard deviation) one independent variable at a time, while the rest of the independent variables were kept at their mean values. The series of the Mr values thus obtained were compared with the primary Mr value. It is also worth pointing out that one-half standard deviation was used instead of one standard deviation because it was found that one standard deviation may change the independent value to an extent beyond the range of the original independent parameters used in this study.

The results of the sensitivity analysis of MLPN model are presented in Table 4. Only unconfined compressive strength followed by moisture content showed significant sensitivity in the MLPN model. These two independent variables had more than a 5% difference in comparison to the Mr values. Free-lime content followed by passing No. 325 sieve of additive, passing No. 200 sieve of additive, SSA of additive, percent of additive, PI of soil, calcium oxide content of additive, Fe2O3 content, loss on ignition, deviatoric stress, SSR of soil-additive mixture had only modest influence (2 – 5 percent) on Mr. Dry unit weight, clay content, pH of soil, CEC, and confining stress had less than 1% difference in the comparison of Mr values. The rank of each independent variable considered here based on the sensitivity result is presented in Table 4. The reason for the low effect of dry unit weight may be that the influence of dry unit weight is overshadowed by other material parameters. Low sensitivity of confining stress is consistent with the observations reported by other researchers.

Concluding Remarks

In this study, a total of two feed-forward-type ANN models, were evaluated to correlate resilient modulus with specimen characteristics and soil/additive properties. An Mr database was developed using laboratory test results on 160 specimens prepared by using four soils stabilized with three additives, namely, lime (3%, 6% and 9%), CFA (5%, 10% and 15%) and CKD (5%, 10% and 15%) was used. Of these, three soils namely, P- (silty clay), V- (lean clay) and C- (fat clay) soil were used in development/evaluation, and the remaining one soil (K-soil, lean clay) was used in the validation of the selected models. The following points highlight the assessments and evaluations of these models:

1. For the RBFN model, with one hidden layer, the R^2 value for the development/evaluation dataset showed worst performance (0.62) among all the ANN models used in this study. Also, it was found that the R^2 value for fewer specimens is close to 1 but the correlation becomes weaker and appears in a "banded" distribution as more soil and additives types are included in the dataset. Further, study showed that RBFN model predicts Mr values of validation dataset with lowest reliability (R^2 = 0.32, Se/Sy = 1.26).
2. The R^2 value of the MLPN model with one hidden layer was found to be 0.99 for evaluation/development dataset. Based on R^2 value and visual examination, this model appeared to be

Table 4. Sensitivity Study for the Neural Network MLP 25-9-1 Model.

Independent Variables	Average[a]	Standard Deviation	Percent Different[b] +	Rank[b] +	Percent Different[c] –	Rank[c] –
Primary M_r (MPa)	889.8	---	---	---	---	---
UCS (kPa)	810.5	543.3	32.72	1	-36.14	1
MC (%)	77.3	43.3	6.34	2	-5.86	2
DUW (kN/m^3)	19.3	4.0	1.30	14	0.13	25
P_{200} (%)	16.5	0.8	-3.04	5	3.65	5
PI	92.8	4.7	3.94	3	-2.96	8
CC (%)	17.6	9.1	0.08	24	-0.59	22
pH_s	37.5	13.6	1.59	9	-0.84	21
SSA_s (m^2/g)	7.3	2.0	-2.67	7	1.03	18
CEC (meq/100g)	98.3	25.6	-1.37	13	0.96	20
PA (%)	14.4	6.9	-3.35	4	3.01	7
SiO_2 (%)	8.4	4.0	0.85	20	-0.99	19
Al_2O_3 (%)	17.8	15.3	-0.24	23	-1.07	17
Fe_2O_3 (%)	7.1	7.4	-1.40	12	-2.47	10
SSR_a	2.7	2.3	-2.59	8	0.28	23
CaO (%)	3.6	1.8	1.26	15	-2.81	9
MgO (%)	46.2	18.0	-0.79	22	-1.89	14
ACA (%)	2.5	1.9	-0.95	17	-1.54	16
FL (%)	1.4	0.9	-0.92	18	-4.23	3
LOI (%)	17.1	20.1	0.97	16	-2.27	11
P_{325} (%)	19.7	13.5	1.47	11	-3.66	4
pH_a	92.7	5.2	2.73	6	-1.81	15
SSA_a	12.3	0.3	0.80	21	-3.36	6
SSR_m	11.6	4.5	0.85	19	-2.12	13
σ_3 (kPa)	10.6	4.5	-0.02	25	0.16	24
σ_d (kPa)	27.6	11.2	-1.55	10	2.12	12

[a]reference value; [b]independent variable plus one-half standard deviation (Note: some plus one standard deviation values are out of variables range); [c]independent variable minus one-half standard deviation.

the best model. Further, validation of MLPN model using a different dataset showed Se/Sy value of 0.60 and R^2 value of 0.96 indicating high quality of Mr prediction achieved by using the MLPN model.

3. Overall, the MLPN model was found to be the best model for the present development/evaluation and validation datasets. This model as well as the other models could be refined using an enriched database.
4. The sensitivity ranking of MLPN model showed that the resilient modulus values are most sensitive to unconfined compressive strength and moisture content. The confining stress, on the other hand, is the least sensitive independent variable for the soils and additives considered in this study.

References

1. AASHTO (1986). Standard Specifications for Transportation Materials and Methods of Sampling and Testing. Washington, DC, USA.
2. Kim, D., and Stokoe, II K.H. (1992). "Characterization of Resilient Modulus of Compacted Subgrade Soils using Resonant Column and Torsional Shear Tests," *Transportation Research Record*, No. 1369, pp. 83 – 91.
3. George, K.P. (1992). "Resilient Testing of Soils using Gyratory Testing Machine," *Transportation Research Record*, No. 1369, pp. 63 – 72.
4. Kim, D., Kweon, G., and Lee, K. (1997). "Alternative Method of Determining Resilient Modulus of Compacted Subgrade Soils Using Free-Free Resonant Column Test," *Transportation Research Record*, No. 1577, pp. 62 – 69.
5. AASHTO (2004). "Guide for Mechanistic-Empirical Design of New and Rehabilitated Pavement Structures," *NCHRP Report 1-37A*, National Cooperative Highway Research Program, Transportation Research Board, National Research Council, Washington DC, USA.
6. Lee, W., Bohra, N.C., Altschaeffl, A.G. and White, T.D. (1998). "Resilient Modulus of Cohesive Soils," *Journal of Geotechnical and Geoenvironmental Engineering*, ASCE, 123(2), pp. 131 – 135.
7. Mohammad, L.N., Huang, B., Puppala, A.J. and Allen, A. (1999). "Regression Model for Resilient Modulus of Subgrade Soils," *Transportation Research Record*, No. 1687, pp. 47 – 54.
8. Ooi, P.S., Archilla, R. and Sandefur, K.G. (2004). "Resilient Modulus Model for Compacted Cohesive Soils," *Transportation Research Record*, No. 1874, pp. 115 – 124.
9. Rahim, A.M., and George, K.P. (2004). "Subgrade Soil Index Properties to Estimate Resilient Modulus," Transportation Research Board 83rd Annual Meeting, CD-ROM Publication, Transportation Research Board, Washington, DC, USA.

10. Elias, M.B. and Titi, H.H. (2006). "Evaluation of Resilient Modulus Model Parameter for Mechanistic-Empirical Pavement Design," *Transportation Research Record*, No. 1967, pp. 89 – 100.
11. Hossain, M.S. (2009). "Estimation of Subgrade Resilient Modulus for Virginia Soil," Transportation Research Board 88th Annual Meeting, CD-ROM Publication, Transportation Research Board, Washington, DC, USA.
12. Mohammad, L.N., Nazzal, M.D., Abu-Farsakh, M.Y. and Alshibli, K. (2009). "Estimation of Subgrade Soils Resilient Modulus from In-situ Devices Test Results," *ASTM Journal of Testing and Evaluation*, 37(3), pp. 1 – 9.
13. Achampong, F. (1996). "Evaluation of Resilient Modulus for Lime and Cement Stabilized Synthetic Cohesive Soils," PhD Thesis, Wayne State University, Detroit, MI, USA.
14. Arora, S., and Aydilek, A.H. (2005). "Class F Fly-Ash-Amended Soils as Highway Base Materials." *Journal of Materials in Civil Engineering*, ASCE, 17(6), pp. 640 – 649.
15. Ling, J., Xie, H., and Guo, R. (2008). "A Method to Predict Resilient Modulus of Lime and Lime-Cement Stabilized Soils Used in Highway Subgrade," Transportation Research Board 87th Annual Meeting, CD-ROM Publication, Transportation Research Board, Washington, DC, USA.
16. Achampong, F., Usmen, M., and Kagawat, T. (1997). "Evaluation of Resilient Modulus for Lime- and Cement-Stabilized Synthetic Cohesive Soils," *Transportation Research Record*, No. 1589, pp. 70 – 75.
17. Hillbrich, S.L., and Scullion, T. (2006). "A Rapid Alternative for Laboratory Determination of Resilient Modulus Input Values on Stabilized Materials for the AASHTO M-E Design Guide," Transportation Research Board 86th Annual Meeting, CD-ROM Publication, Transportation Research Board, Washington, DC, USA.
18. Mooney, M.A. and Toohey, N.M. (2010). "Accelerated Curing and Strength-Modulus Correlation for Lime-Stabilized Soils," Final *Repot No. CDOT-2010-1*, Colorado Department of Transportation, Denver, CO, USA.
19. Transportation Research Board (1999). "Use of Artificial Neural Networks in Geomechanical and Pavement Systems," Transportation research circular number E-C012, Transportation Research Board, National Research Council, Washington, DC, USA.
20. Najjar, Y.M., Basheer, I.A., Ali, H.E., and McReynolds, R.L. (2000). "Swelling Potential of Kansas Soils: Modeling and Validation Using Artificial Neural Network Reliability Approach," *Transportation Research Record*, No. 1736, pp. 141 – 147.
21. Shahin, M.A., Maier, H.R., and Jaksa, M.B. (2004). "Data Division for Developing Neural Networks Applied to Geotechnical Engineering," *Journal of Computing in Civil Engineering*, 18(2), pp. 105 – 114.
22. Zaman, M., Solanki, P., Ebrahimi, A., and White, L. (2010). "Neural Network Modeling of Resilient Modulus Using Routine Subgrade Soil Properties," *International Journal of Geomechanics*, ASCE, 10(1), pp. 1 – 12.
23. Zurada, J.M. (1992). *Introduction to Artificial Neural Systems*, West St. Paul, MN, USA.
24. Fausett, L.V. (1994). *Fundamentals neural networks: Architecture, Algorithms and Applications*, Prentice-Hall, Inc, Englewood Cliffs, NJ, USA.
25. Ripley, B.D. (1996). *Pattern Recognition and Neural Networks*, Cambridge University Press, Cambridge, UK.
26. Hill, T., and Lewicki, P. (2006). *STATISTICS Methods and Applications*. StatSoft, Tulsa, OK, USA.
27. StatSoft Inc. (2006). *Electronic Statistics Textbook*. Tulsa, OK, USA.
28. Sharma, S., and Das, A. (2008). "Backcalculation of Pavement Layer Moduli from Falling Weight Deflectometer Data Using an Artificial Neural Network," *Canadian Journal of Civil Engineering*, 35(1), pp. 57 – 66.
29. Far, M.S.S., Underwood, B.S., Ranjithan, S.R., Kim, Y.R., and Jackson, N. (2009). "The Application of Artificial Neural Networks for Estimating the Dynamic Modulus of Asphalt Concrete," Transportation Research Board 2009 Annual Meeting, CD-ROM Publication, Washington, DC, USA.
30. Skapura, D.M. (1996). *Building Neural Networks*. ACM Press, NY, USA.
31. Shahin M.A., Jaksa, M.B., and Maier, H.R. (2001). "Artificial Neural Network Applications in Geotechnical Engineering." *Australian Geomechanics*, 36(1), pp. 49 – 62.
32. Meier R.W., Alexander, D., and Freeman, R.B. (1996). "Using Artificial Neural Networks as a Forward Approach to Backcalculation," *Transportation Research Record*, No. 1570, pp. 126 – 133.
33. Ceylan, H., Schwartz, C.W., Kim, S., and Gopalakrishnan, K. (2009). "Accuracy of Predictive Models for Dynamic Modulus of Hot-Mix Asphalt," *Journal of Materials in Civil Engineering*, 21(6), pp. 286-293.
34. Xiao, F., and Amirkhanian, S.N. (2009). "Artificial Neural Network Approach to Estimating Stiffness Behavior of Rubberized Asphalt Concrete Containing Reclaimed Asphalt Pavement," *Journal of Transportation Engineering*, 135(8), pp. 580-589.
35. Xiao, F., Putman, B.J., and Amirkhanian, S.N. (2010). "Viscosity Prediction of CRM Binders Using Artificial Neural Network Approach," *International Journal of Pavement Engineering*, 12(5), pp. 485 – 495.
36. Far, M.S.S., Underwood, B.S., Kim, Y.R., Puccinelli, J. and Jackson, N. (2010). "Development of Artificial Neural Network Predictive Models for Populating the Dynamic Moduli of LTPP Sections," Transportation Research Board 89th Annual Meeting, CD-ROM Publication, Transportation Research Board, Washington, DC, USA.
37. Thube, D.T. (2012). "Artificial Neural Network (ANN) Based Pavement Deterioration Models for Low Volume Roads in India," *International Journal of Pavement Research and Technology*, 5(2), pp. 115 – 120.
38. Solanki, P. (2010). Characterization of Cementitiously Stabilized Subgrades for Mechanistic-Empirical Pavement Design, Ph.D. Dissertation, University of Oklahoma, Norman, OK, USA.
39. Cerato, A.B. and Lutenegger, A.J. (2002). Determination of surface are of fine-grained soils by the ethylene glycol monoethyl ether (EGME) method, *ASTM Geotechnical Testing*

Journal, 25(3), pp. 1 – 7.

40. Tarefder R.A., White L., and Zaman, M. (2005). “Neural Network Model for Asphalt Concrete Permeability,” *Journal of Materials in Civil Engineering*, ASCE, 17(1), pp. 19 – 27.
41. Rankine, R.M., and Sivakugan, N. (2005). “Prediction of Paste Backfill Performance Using Artificial Neural Networks,” *Proceedings of the 16th ISSMGE*, Vol. 2, Osaka, Canada, pp. 1107-1110.
42. Solanki, P., Ebrahimi, A., and Zaman, M.M. (2008). “Statistical Models for Determination of the Resilient Modulus of Subgrade Soils,” *International Journal of Pavement Research and Technology*, 1(3), pp. 85 – 93.
43. Haykin, W.L. (1994). *Neural Networks: A Comprehensive Foundation*. Macmillan College Publishing, NY, USA.
44. Bishop, C. (1995). *Neural Networks for Pattern Recognition*, University Press, Oxford, United Kingdom.
45. Rumelhart, D.E., and McClelland, J. (1986). *Parallel Distributed Processing*. Vol. 1, MIT Press, Cambridge, MA, USA.
46. Narayan, S. (2002). “Using Genetic Algorithms to Adapt Neuron Functional Forms,” *Proceedings Artificial Intelligence and Soft Computing*, Banff, Canada, pp. 299-302.
47. Montgomery, D.C., Peck, E.A., and Vining, G.G. (2006). *Introduction to Linear Regression Analyses. Wiley Series in Probability and Statistics*, John Wiley and Sons, Inc, Hoboken, NJ, USA.
48. Myers, R.H., Montgomery, D.C., and Vining, G.G. (2001). *Generalized Linear Models: With Applications in Engineering and the Sciences*, John Wiley and Sons, Inc, Hoboken, NJ, USA.